JP6.3 Plume Rise and Ground-Level Concentration of Emission from a Distributed Power Generation Unit: Field Observations and Water Channel Modeling

Xiangyi Li*, S. Chen, M. Princevac, A. Venkatram, D. Pankratz, and C. Bartolome
Laboratory for Environmental Flow Modeling
University of California at Riverside, Riverside, California, USA

1. INTRODUCTION

Distributed Generation (DG) plays an important role in making use of small distributed sources to produce electrical power or combined heat and power to serve neighborhoods and businesses. There were various reasons that DG is considered as a high efficiency, low pollution solution (Grubb et al., 1999; MacCracken et al., 1999) to the deteriorating energy situation, however, further researches suggested that DG may lead to increased level of in-basin pollutants and adversely impact the air quality (Allison and Lents, 2002, Rodrigues, M.A. et al., 2006). Therefore, the impact of DGs on air quality needs to be carefully evaluated to meet federal and state regulations. Most regulatory air quality models designed to estimate the impact of central power plants in rural areas have difficulty in predicting the impact of DGs in more complex urban areas. With a goal to improve the quality of regulatory models, field and laboratory experiments were conducted to advance the understanding of pollutant dispersion from a DG in an urban environment.

A dispersion study took place in Palm Springs, California, in July 2008, to investigate DG's impact on urban environment. The tracer gas, SF6, was collected through 49 sampling facilities located in arcs surrounding DG. Meteorological data including wind velocity, temperature, heat fluxes, and radiation were recorded. To complement the field measurements a scaled laboratory simulation was conducted at the Laboratory for Environmental Flow Modeling (LEFM) at UC-Riverside.

* *Corresponding author address*: Xiangyi Li, Univ. of California, Riverside, Dept. of Mechanical Engineering, Riverside, CA 92521; e-mail: xli0@engr.ucr.edu

2. FIELD STUDY

A 650 KW reciprocating generator is located in a typical southwestern urban setting. The tracer gas, SF6, was released from the exhaust stack of the DG, and the ground-level concentrations were recorded at 49 tracer sampler locations. A total of seven, three day-times and four night-times, dispersion experiments were conducted. (See Fig. 1) We applied two sets of instruments for collecting meteorological data. The first set was mounted on a tower in a parking lot located approximately 75 meters from the source and the second set at the roof of the DG site, next to the exhaust stack.

3. LABORATORY SETUP

3.1 Mock Buildings and Facilities

A scale-down urban setting of DG and surrounding buildings was constructed in a laboratory water channel. The stack height, here the distance from the top of the stack to the ground level, is 3.1 cm, 300 times smaller than the stack height in the real world (9.3 m). Thus the 1.5m x 1m x 0.5m test section in the water channel represents a space of 450m x 300m x 150m in the real world. Since there is no other significant building within 100 m of the DG building, we focused only on two immediately adjacent buildings, which were also built from acrylic blocks with a scale of 1:300, modeled in

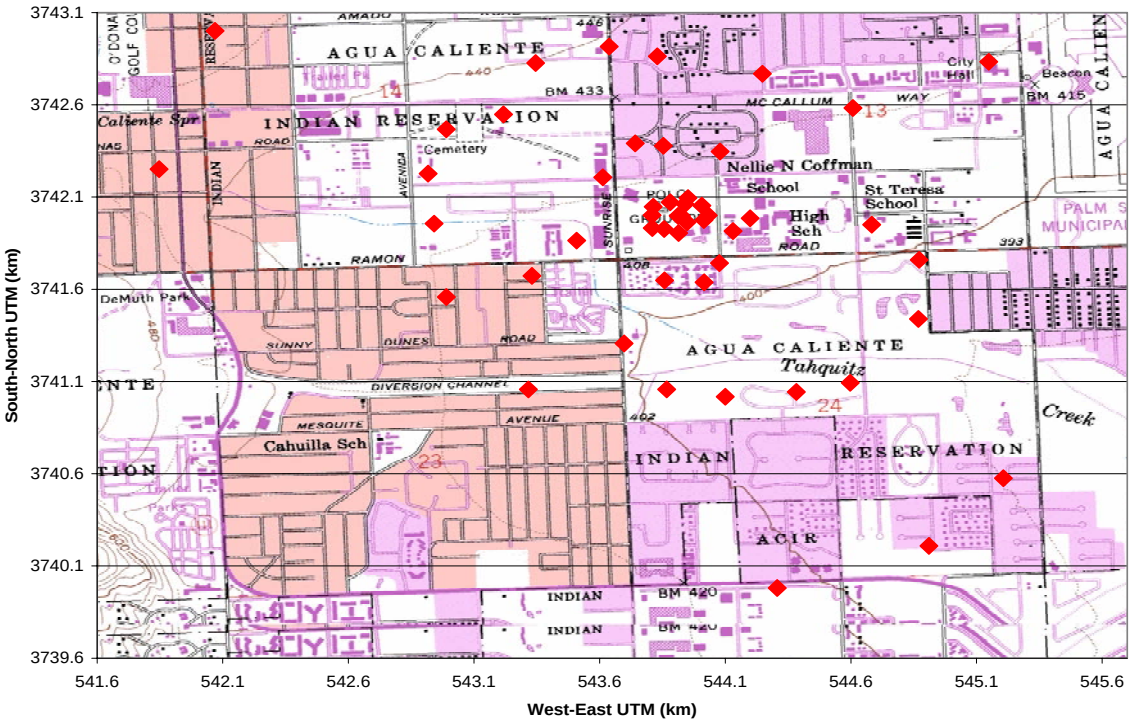

Fig. 1 Field measurement sampling locations (Venkatram, A., et al., 2008)

the water channel. The incoming flow conditions are logarithmic profiles with a mean free-stream flow speed of 0.04 m s^{-1}. In order to keep the same turbulence intensities, σ_w/U, as in the field, an array of Lego blocks was introduced before the buildings to increase σ_w/U from ~20% to ~36%. A gear pump connected with plastic tubing served as a source feeding system. It injects the Uranine green dye, for visualization or the Rhodamine B (hereafter Rhodamine) dye, for quantitative concentration measurements. The buoyancy and flow rate of the initial plume source was determined by similarity between the field and the laboratory conditions. The buoyant plume rise was estimated from dye visualization. The velocity field and the concentration distribution were measured by Particle Image Velocimetry (PIV) and Planar Laser-Induced Florescence (PLIF) respectively.

3.2 Similarity Principals

As a first step of the laboratory simulation of pollutant dispersion a similarity criteria have to be satisfied by proper scaling of geometry, velocity (kinematic similarity) and forces (buoyancy similarity), as presented in equations (1) thru (3):

$$\left(\frac{D}{L}\right)_L = \left(\frac{D}{L}\right)_F \quad (1)$$

$$\left(\frac{V_s}{U}\right)_L = \left(\frac{V_s}{U}\right)_F \quad (2)$$

$$\left(\frac{\Delta h}{L}\right)_L = \left(\frac{\Delta h}{L}\right)_F \quad (3)$$

where D is the exhaust diameter, V_s is the stack velocity, U is the ambient wind velocity, Δh is the plume rise from the stack height L. Equation (1) is solved for the diameter for laboratory model to be 1mm. To preserve the turbulent nature of the plume near the source we relaxed the geometric similarity by allowing the stack diameter to be 2

mm to double the Reynolds number of the source flow. The kinematic similarity defined the flow rate of the plume. In (3), starting from Brigg's 2/3 law it can be shown that the final plume rise is given as:

$$\Delta h = 1.8\frac{F}{U\sigma_w^2} \tag{4}$$

And buoyancy flux parameter *F* for laboratory is:

$$F_L = \frac{gV_sD^2}{4}\frac{\rho_0-\rho_s}{\rho_0} = \frac{gV_sD^2}{4}(1-SG) \tag{5}$$

where q is the gravitational acceleration, ρ_0 is the ambient density, ρ_s is the source plume density and *SG* is the specific gravity. To meet the calculated specific gravity of the source, alcohol and water were mixed with dye according to the desired ratio. Moreover, by satisfying (3), the influence of the diameter on the buoyancy flux also was corrected. After all laboratory parameters are determined, the measured concentration, expressed as dilution *d*, in the water channel can be converted to the field scale as

$$\frac{d_F}{d_L} = \frac{(C/C_0)_F\,\dot{Q}_L}{(C/C_0)_L\,\dot{Q}_F} = \left(\frac{L_LD_F}{L_FD_L}\right)^2\left(\frac{D_L{}^2V_L}{D_F{}^2V_F}\right)$$

$$= \frac{V_LL_L{}^2}{V_FL_F{}^2} = \frac{U_LL_L{}^2}{U_FL_F{}^2} \tag{6}$$

where *C* is concentration, C0 is concentration at the source, and $\dot{Q}$ is the source volumetric flow rate. Once the laboratory dilution has been obtained, the field dilution as well as the field concentration can be obtained from Equation (6).

4. RESULTS

4.1 Plume Rise and Plume Structure

Plume rise is the combined result of the initial buoyancy, momentum as and the interaction with the ambient flow. Also, numerous previous empirical evidences showed that plume rise affects the ground-level concentration the most. Brigg's equation for plume rise is widely accepted and agrees with the numerous realistic cases. From the concentration field, we can also exam the vertical plume spread, σ_z. The black dotted lines in Figures 2 (b-d) represent the vertical plume spread σ_z integrated from vertical concentration profile as:

$$\sigma_z^2 = \frac{\int_0^\infty z^2Cdz - \left(\int_0^\infty zCdz\right)^2}{\int_0^\infty Cdz} \tag{7}$$

In our results, the measured concentration field offered us the advantage to directly find the maximum concentration at any downwind distance from the source. The results have a good agreement with Brigg's formula (Brigg, 1975) (Fig. 2) as:

$$\Delta h = 1.6\frac{F^{1/3}x^{2/3}}{U} \tag{8}$$

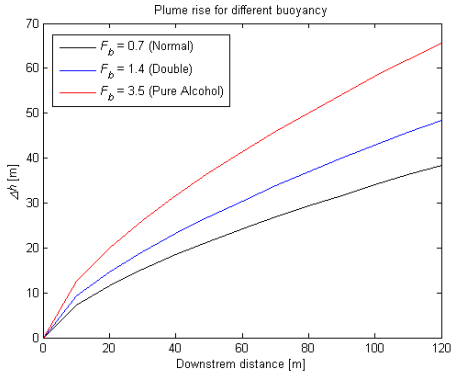

Fig. 2(a) Brigg's 2/3 law of plume rise for different buoyancy cases

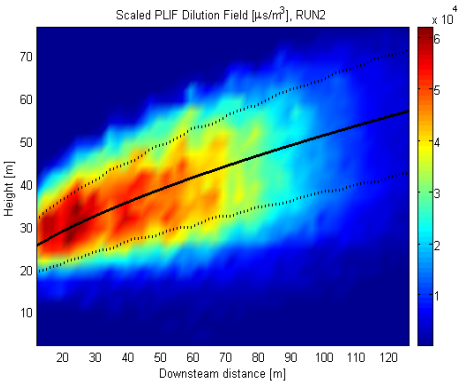

Fig. 2(b) Laboratory measurements of the plume for SG=0.96,F_b=0.7 m^4/s^3 case. Solid black line presents Brigg's 2/3 law and dotted lines are calculated σ_z.

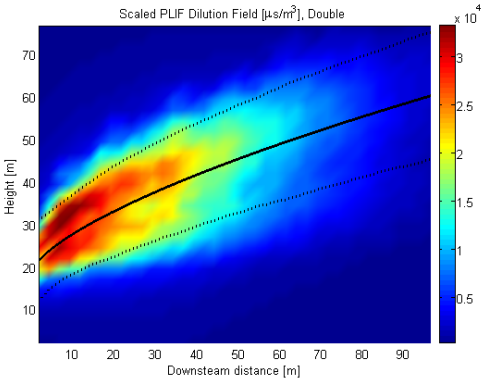

Fig. 2(c) Plume rise and dispersion for SG=0.91,F_b=1.4 m^4/s^3 case

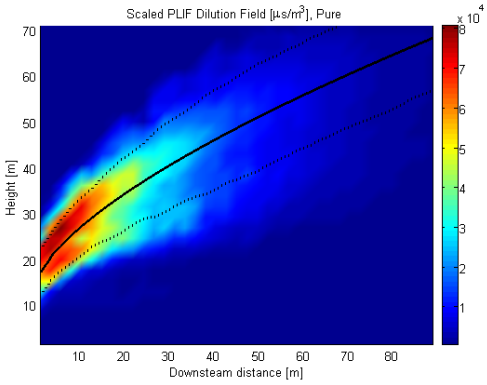

Fig. 2(d) Plume rise and dispersion for SG=0.8, F_b=3.5 m^4/s^3 case

In order to investigate the vertical plume structure, we plot vertical concentration profile at different downwind locations (Fig. 3). Note that the plume core does not follow expected Gaussian curvature but the concentration in the core region it is rather constant. This presents the first detailed concentration measurements of the whole plume structure.

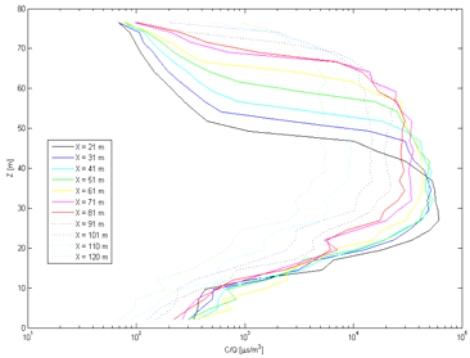

Fig.3 Vertical Concentration profiles at different down-wind locations on y=0 (central) plane

From Fig. 3, we observed that the maximum concentration doest not only exist at the plume center-line level (which was assumed by Gaussian distribution), but includes a wider range vertically and the range extends to as wide as the whole plume dispersion range in vertical direction. Possible explanation for this observed constant concentration in the core can be enhanced mixing due to the formation of double-vortex structure (Fig. 4). The double-vortex is caused by the buoyancy force lifting the core in the middle of the cross section and downward friction force exerted on the outer region of the plume. With the help of the PIV/PLIF technique, it is now feasible to investigate the plume structure in further detail. The maximum concentration in the core decays with downstream distance.

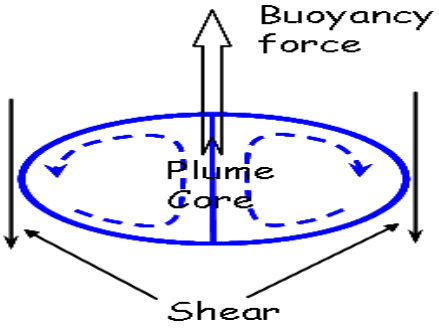

Fig.4 Double-vortex structure (Venkatram, A., et al., 2008)

4.2 Ground-Level Concentration (GLC)

The PLIF is an adequate tool to capture details of the concentration field and key parameters such as the plume rise and the plume spread. However, there are certain difficulties in determining the GLC. The challenge here is that GLC is usually several orders of magnitudes smaller than source concentration and can easily be within the noise level compared to the maximum concentration. Another difficulty in measuring the GLC is the possibility of enhanced laser illumination due to the laser light reflection from the ground. For these reasons a special care has to be taken when measuring GLC. By avoiding illumination of the source, where the highest concentration occurs, and preventing laser light ground reflection the GLC was successfully measured and compared to the field measurement. (Fig. 5)

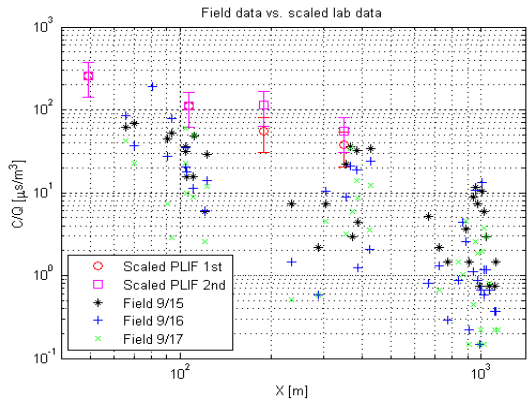

Fig. 5 GLC Laboratory measurements compared with field data

Fig. 5 shows the sets of GLC results from 2 runs up to a downwind distance of 350 m (both with PLIF only, 2 mm stack diameter and using Rhodamine). Each laboratory data point represents the averaged value of GLC over distance in a measuring window. This averaging helps to compensate for the non uniformity of the laser sheet intensity, i.e., laser intensity is stronger around the center and weaker on the side. Therefore, by carefully adjusting the spread angle of the laser and averaging the concentration in every screen, we effectively avoid 'artificial' peak caused by the non-uniformity in the laser light density. Since we are interested in the trend of the GLC with distance, averaged results are thus acceptable. This laser sheet non uniformity can be significant in measuring low concentration levels as in GLC. In Figure 4, we can see that the scaled PLIF data do follow the trend of the field data, taken from the three day-time releases in the Palm Springs Field Study. These results validate the PLIF measuring technique and our scaling laws.

5. SUMMARY, CONCLUSIONS AND DISCUSSION

This case study, through scaled laboratory simulation for Palm Springs' DG station at LEFM, shows the trends of the ground-level concentration that agree with the field ground-level measurements. This allows for future investigation of the impact of DG and similar dispersion problems in an approach less expensive than field measurements. The remaining difficulties include how to quantify the difference of the laser intensity and the contamination caused by the higher concentration fluorescence while measuring GLC. The laboratory experiments for the first time revealed detailed plume structure and the region of constant concentration in the plume core which is hypothesized to be a consequence of the double vortex formation driven by buoyancy and shear forces. Future researches

will extend to: (1) estimate near-source dispersion; (2) understand effects on ground-level concentration due to plume rise; (3) understand the effects on plume rise and ground-level concentration due to variety of surrounding building complex; (4) understand the interaction between buoyancy induced turbulence and ambient turbulence.

REFERENCES

Allison, J.E., Lents, J., 2002: Encouraging distributed generation of power that improves air quality: can we have our cake and eat it too? *Energy Policy*, 30: 737-752

Brigg, G.A., 1975: Plume Rise Predictions, in *Lecture on Air Pollution and Environmental Impact Analyses*, Workshop Proceedings, Boston, Mass., Sept. 29- Oct. 3, 1975, pp. 59-111, American Meteorological Society, Boston.

Grubb, M., Vrolijk, C., Brack, B., 1999: The Kyoto Protocol: a guide and assessment. Royal Institute of International Affairs, London.

MacCracken, C., Edmonds, N., Kim, A.J.S.H., Sands, R.D., 1999: The economics of the Kyoto Protocol. In: Weyant, J.P. (Ed.), The Costs of the Kyoto Protocol: A Multi-Model Evaluation Cleaveland, *Energy Journal*/International Association for Energy Economics ISSN 0195-6574.

Rodriguez, M.A., et al., 2006: Air quality impacts of distributed power generation in the South Coast Air Basin of California 1: Scenario development and modeling analysis, *Atmospheric Environment*, 40: 5508-5521.

Venkatram, A., et al., 2008: Estimating Air Quality Impacts in Urban Neighborhoods from the Use of Distributed Generation. Presented in: California Energy and Air Quality Conference.